IEEE Photonics Journal
An IEEE Photonics Society Publication

Open Access

Continuously Tunable Optical Notch Filter With Functions of a Mirror and a Beam Splitter

Volume 11, Number 1, February 2019

Mi-Yun Jeong
Keumcheol Kwak

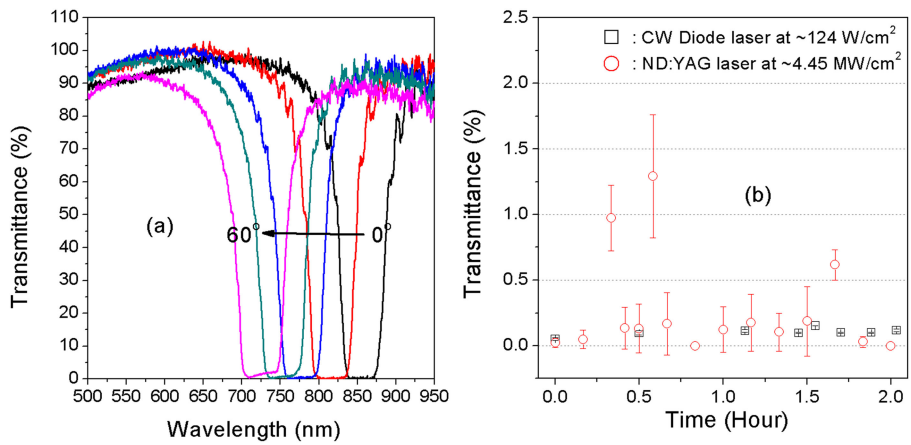

DOI: 10.1109/JPHOT.2018.2885314
1943-0655 © 2018 IEEE

Continuously Tunable Optical Notch Filter With Functions of a Mirror and a Beam Splitter

Mi-Yun Jeong [1] **and Keumcheol Kwak** [2]

[1]Department of Physics and Research Institute of Natural Science, Gyeongsang National University, Jinju 52828, South Korea
[2]School of Electronics and Electrical Engineering, Sungkyunkwan University, Suwon 16419, South Korea

DOI:10.1109/JPHOT.2018.2885314

Manuscript received October 31, 2018; revised November 30, 2018; accepted December 1, 2018. Date of publication December 6, 2018; date of current version December 28, 2018. This work was supported by a grant (2017R1D1A1A02019309) of the Basic Science Research Program through the National Research Foundation funded by the Ministry of Science, ICT and Future Planning, Republic of Korea.
Corresponding author: Mi-Yun Jeong (e-mail: jmy97@gnu.ac.kr).

Abstract: The objective of this study was to develop continuously tunable optical notch filters by combining four left- and right-handed circular cholesteric liquid crystal (CLC) cells without subsidiary optical components. By rotating each filter, the photonic band position could be continuously blue shifted over 100-nm spectral range. Using four notch filter sets with four different chiral dopant concentrations, spectral range from 440 to 870 nm could be covered. Since each CLC cell has only one chiral dopant concentration, it could be stable for a long time. Each filter is independent of polarization in the spectral range. Filter performance was highly enhanced by introducing an anti-reflection layer on the filter device. There was no light leakage inside the photonic band. Outside the band, transmittance was about 70%–100%. In addition, these filters had stable operation under extremely high laser intensity (∼124 W/cm^2 of CW 532-nm diode laser and ∼4.43 MW/cm^2 of Nd: YAG pulse laser operation for 2 h) without showing damage. Such filters also have functions as a mirror and a beam splitter. Depending on CLC materials, this simple and easy strategy could be used to prepare filters for applications in VIS and NIR spectral range devices.

Index Terms: Tunable optical filters, continuous tunable filter, liquid crystal filter, optical devices, photonic crystal.

1. Introduction

Tunable optical filters are essential components of various devices to selectively manipulate optical signals in broad UV, VIS, and NIR spectral range, including imaging Raman spectroscopy, multi-photon microscopy, laser-based fluorescence, astronomical telescopes, and supercontinuum lasers, biomedical applications and optical communication systems. Thus, various kinds of tunable optical filters have been developed by controlling the refractive index or the birefringence of electro-optic materials [1]–[10]. Among them, cholesteric liquid crystals (CLCs) have been intensively studied to develop tunable filters [6]–[10], tunable laser devices [11]–[14], multichannel photonic devices for optical communication [15], [16] and reflective color display devices [17], [18] due to their great potential in optical devices applications. CLCs are one dimensional chiral photonic crystal with self-assembled periodic helical nano structure which consists of nematic liquid crystals (NLC)

and chiral molecules. One of the unique optical properties of CLC is Bragg reflection. For circularly polarized light having the same handedness as that of the CLC, a selective reflection occurs in the central wavelength $\lambda = n \times p$ with bandwidth $\Delta\lambda = |n_e - n_0| \times p$, where n is the average reflective index, pitch (p) is the length for one full rotation of the director around the helix axis and n_o and n_e are ordinary and extraordinary refractive indices of the liquid crystal, respectively, [6]–[14], [17], [18]. Optical characteristic properties of CLCs such as pitch and birefringence of nematic liquid crystal ($\triangle$n) of CLCs could be controlled by changing chiral dopant concentration [19], temperature control [12], [20], UV curing [21]–[25], and applying an electric field [26]–[28]. By adjusting the birefringence of nematic liquid crystal, n_o and n_e, photonic band gap (PBG Bragg reflection) width could be controlled.

In our previous study, we have achieved continuously tunable and bandwidth variable optical notch and band-pass filters with spectral range from ~460 nm to ~1000 nm by combining cholesteric liquid crystal wedge cells with pitch gradient [10]. However, there was light leakage of ~3% inside the band of filters while transmittance outside the band was low (from 70% to 40%). And to make well-developed pitch gradient in the wedge CLC cell [10], long time, at least two months is required. Furthermore, the developed pitch gradient in the CLC cell has no good long-time stability. To enhance contrast of the filter and overcome disadvantages of previous filters with pitch gradient, the objective of this study was to develop a new strategy to obtain continuously tunable optical notch filters with high performance by introducing an anti-reflection layer on the filter device and by combining four left- and right-handed circular CLC parallel cells with one pitch. The wavelength tuning mechanism of the filter is just rotation of CLC cells. Over 100 nm spectral range without band deformation, the filter performance was very high. As a result, employing CLC cells with four different chiral dopant concentrations at spectral range from 440 nm to 870 nm could be covered. Key advantages of this new strategy are that CLC filters are taking only one chiral dopant concentration without taking a long time to form a pitch gradient and that stability of the filter can be secured for a long period of time. Furthermore, compared to other strategies that require onerous additional instruments systems for temperature control [12], the UV curing [21]–[25], and applying an electric field [26]–[28], our new strategy is very simple in setup because only one rotator is needed for tuning the wavelength position of the filter. In addition, wavelength position of the filter can be exactly controlled reversibly by adjusting the rotation angle of the CLC cell. Moreover, there is no deformation of the helical nano structure by external forces such as electric fields or temperature. Experimentally measured data fitted well with theoretically calculated data using the 4×4 matrix method [29]–[31], thus confirming the exactly tuned band wavelength position by rotation of the filter. To the best of our knowledge, wavelength tunable notch filter with spectral range over 100 nm without band deformation by rotation has not been previously reported. Another very interesting result was that these filters had stable operation under extremely high laser intensity (~124 W/cm^2 of CW 532 nm Diode laser and ~4.43 MW/cm^2 of Nd: YAG pulse laser operation for two hours) without showing damage. These filters also had functions as a Mirror and an intensity variable Beam Splitter. Such filters not only could be applied to a broad spectra range and high power laser intensity but also offer low cost with dramatically simple fabrication process, simple mechanical control, and small size. Thus, this strategy could be utilized to prepare filters for various applications in devices with VIS and NIR spectral range.

2. CLC-Cell Fabrication

Properties of the substrate that makes up the filter can affect the transmittance and reflectance of the filter. To compare effects of three different substrates, BK7 plates, BK7 plates coated with anti-reflection layer on one side, and soda lime (SL) plates coated with ITO layer on one side were used. Anti-reflection (AR) coating on BK7 plate was done with 0.6 μm thickness (Yunam Optics Co., Korea, detailed coating conditions correspond to trade secretes) at spectral range from 400 nm to 1000 nm. Liquid crystal alignment layer of polyimide (PI) (SE-5291, pretilt angle of 6°~7°, Nissan Chemical Korea Co. Ltd., Korea) was spin coated on BK7 and ITO surfaces of plates, resulting in fabrication of three kinds of multilayer plates; PI/BK7, PI/BK7/AR-layer, and PI/ITO/SL. After the PI

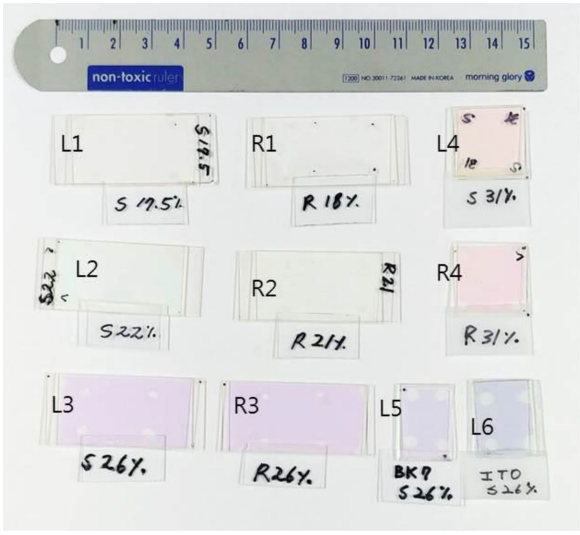

Fig. 1. Photographic images of fabricated L-CLC cells using S811 (L1;17.5 Wt.%, L2; 22 Wt.%, L3; 26 Wt.%, and L4; 31 Wt.%) and R-CLC cells using R811 (R1; 18 Wt.%, R2; 21 Wt.%, R3; 26 Wt.%, and R4; 31 Wt.%) with different chiral dopant concentration made by PI/BK7/AR-layer plates. L-CLC cells of S811 (26 Wt.%), L5 and L6 were made by PI/BK7 and PI/ITO/SL plates, respectively.

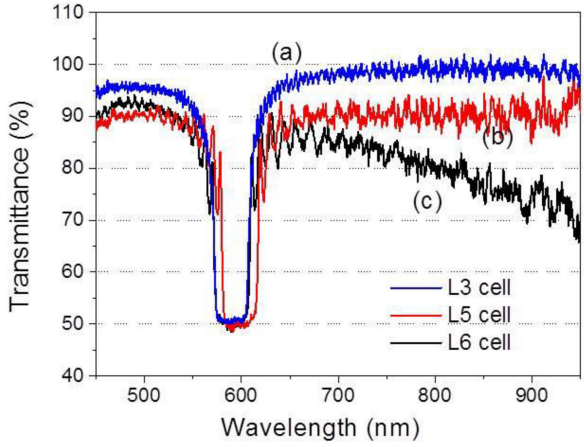

Fig. 2. 3 photonic band gaps: the 3 L-CLC cells have the same chiral molecular (S811) concentration of 26 wt%. L3 was made by PI/BK7/AR-layer plates, L5 was made by PI/BK7 plates, and L6 was made by PI/ITO/SL plates.

layer was thermally treated for crosslinking, PI layer was rubbed with rubbing cloth (HC20, cotton, NESTECHNOLOGY Co., Ltd, Korea). To check the effect of these three different substrates, we made three parallel left-handed circular CLC cells (L-CLC) by the capillary method. They were filled with the same chiral molecular concentration of S811 (26 Wt. %) CLC. However, cells were made by three different kinds of multilayered plates: L3 ($\sim$30 μm thickness), L5 ($\sim$10 μm thickness), and L6 ($\sim$10 μm thickness) cells by PI/BK7/AR-layer plates, PI/BK7 plates, and PI/ITO/SL plates, respectively (Fig. 1). We then compared their PBGs and transmittance (Fig. 2). To study tunable filter, empty parallel cells ($\sim$30 μm thickness) were fabricated using plates of PI/BK7/AR-layer ($\sim$22 mm $\times$ 45 mm $\times$ 1 mm). Eight CLCs with different left- and right-handed chiral dopant concentrations were then filled to cells by capillary method. Left-handed circular CLC cells (L-CLC) and right-handed circular CLC cells (R-CLC) were filled by mixing nematic liquid crystal MLC6608 and chiral material S811 for left-handed circular helicity and chiral material R811 for right-handed circular helicity (all from Merck, Korea), respectively. To cover broad VIS to NIR spectral range, concentrations of

chiral dopants of the CLCs were adjusted to have PBG center wavelength positions at 853 nm (L1; 17.5 Wt. % and R1; 18 Wt. %), 708 nm (L2; 22 Wt. % and R2; 21 Wt. %), 589 nm (L3 and R3; 26Wt. %), and 528 nm (L4 and R4; 31 Wt. %) at room temperature (Fig. 1). To check the stability of filters for high laser power of CW Diode laser and ND: YAG laser with 532 nm wavelength, we additionally made L-CLC (S811, ∼30 wt. %) cells and R-CLC (R811, ∼30 wt.%) cells with ∼10 μm and ∼30 μm thickness by using PI/BK7/AR-layer plates so that PBG center positions were at ∼532 nm. Transmitted band spectra of CLC cells and filters were measured by a spectrometer with a resolution of 0.36 nm (HR 2000+, Ocean Optics, USA).

3. Experimental Results and Discussion

Fig. 2 shows transmittances of three parallel CLC cells with the same L-CLC material but made by three different substrates using PI/BK7/AR-layer plates (L3), PI/BK7 plates (L5), and PI/ITO/SL plates (L6). When transmittance behaviors of these three CLC cells were compared, L3 was relatively superior to L5 and L6. Inside the band near 590 nm, the reflectance of all cells was approximately 50%. However, despite the same CLC concentration was used in each cell, the PBG position of the curve differed by ∼10 nm (comparing a, b, and c curves in Fig. 2). These PBG differences caused by boundary condition of the cell, or cholesteric helical pitches were quantized by the number of half turns between two substrates of the cell [11]–[13], [29]. Outside the band, there was large difference in transmittance. The transmittance of the L5 cell without the AR-layer was ∼90% over the spectral range whereas the transmittance of the L3 cell with the AR-layer was approximately 95% around 450 nm∼600 nm and ∼100% at spectral range over 600 nm. The PI/ITO/SL plate has been widely used for CLC cell fabrication due to its good flatness and ease with using electrodes [11], [26]. Therefore, we also compared transmittance of previous CLC cells. The transmittance outside the band dramatically decreased from 90% to 65% when wavelength was increased (Fig. 2c). This serious behavior is due to refractive index mismatch between neighboring layers of the CLC/PI/ITO/SL/air of the substrate. In our previous filter devices, similar results have been obtained with notch filter and band-pass filter [10]. Thus, the transmittance is not only influenced by the CLC material, but also influenced by the boundary condition of the layers of the cell. As seen in Fig. 2, the AR-layer on BK7 (or glass) substrate could improve the refractive index mismatch between air and glass layers of the CLC cell. We can conclude that the AR-layer on the surface of BK7 CLC cells is a vital factor to greatly improve transmittance and solve light leakage problem in the notch filter. To study tunable filter, CLC cells were then all fabricated with PI/BK7/AR-layer plates. Moreover, near the PBG edges of L5 and L6 cells with thickness of ∼10 μm, there were large oscillations in transmittance. In contrast, there was small oscillation in transmittance of L3 cell whose thickness was ∼30 μm. To remove unnecessary oscillation near the PBG, the required cell thickness is approximately ∼30 μm [10].

Fig. 3a shows experimental setup for measuring the transmittance of the CLC cells and the notch filter. For the notch filter, 1-set CLC notch (including an L-CLC cell and an R-CLC cell and a waveguide W1 of 400-μm diameter) or 2-set CLC notch (including two L-CLC and two R-CLC cells and W1) was employed. To change the wavelength position of band of filters, these CLC cells were rotated with a rotator. Light signals from these cells were acquired through waveguides using spectrometer (USB2000+). A CLC cell structure with AR-layer on BK7 is shown in Fig. 3b. Fig. 3c shows measured transmittances of L-CLC cells (L1, L2, L3 and L4) and R-CLC cells (R1, R2, R3 and R4).

Previously, it has been reported that the PBG position of CLC could be blue shifted upon rotation [29]. In the present study, we employed this blue shift behavior of CLC cells in order to obtain a continuously tunable notch filter. First, we examined changes in PBG position upon rotation of the L-CLC cell (L2) in Fig. 1. Fig. 4(a) shows three PBG data points that are blue shifted and the FWHM of PBGs that are almost unchanged at oblique incident angle of 0° (□), 30° (○), or 50° (△).

Solid lines are of theoretical fitting using Berreman's 4 × 4 matrix method [29]–[31]. At incident angle of 0°, fitting parameters of L2 cell with the structure of Fig. 3b at central wavelength of 597 nm of the Bragg reflection are as follows: for L-CLC, thickness of 30 μm, ordinary refractive

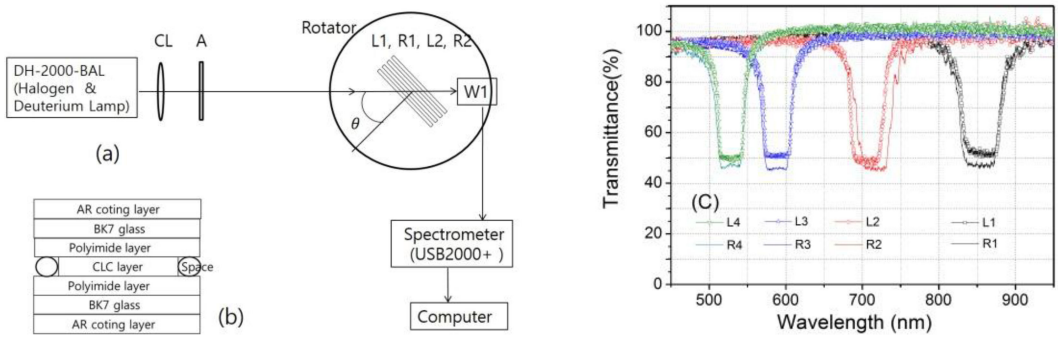

Fig. 3. (a) Experimental set up for the transmittance and notch filters. CL, lens for a collimated beam; A, aperture; L1 and L2, L-CLC cells; R1 and R2, R-CLC cells; W1, waveguide of 400 μm diameter. (b) A CLC cell structure with AR coating layer. (c) Transmittances of (L1, R1), (L2, R2), (L3, R3), and (L4, R4) cells, respectively.

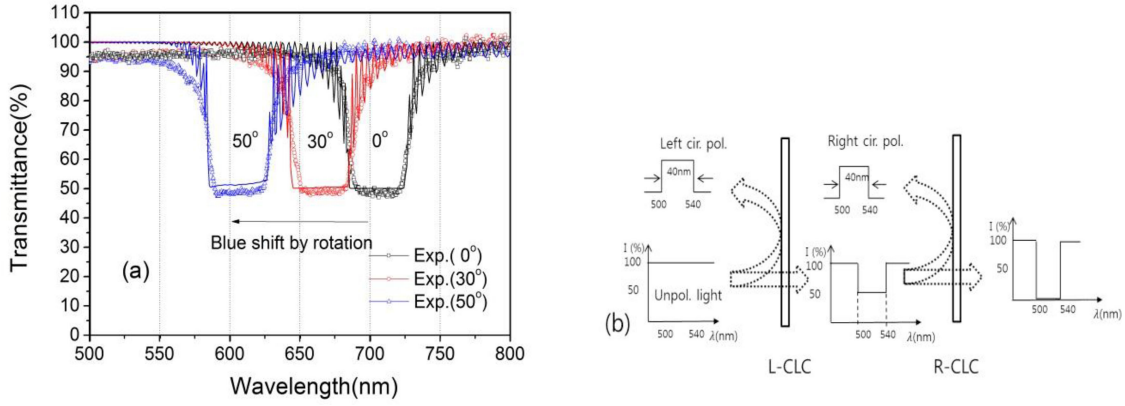

Fig. 4. (a) Blue shift of PBGs for oblique incident angle changes of L2 cell. Three experimentally measured data points at incident angles of 0° (□), 30° (○), and 50° (△) and three theoretical fitting (solid lines) data points are shown. (b) Principle of a notch filter: for unpolarized incident light, left circularly polarized light in the PBG is reflected at L-CLC and right circularly polarized light in the PBG is reflected at R-CLC, in turn.

index (n_o) of 1.4730, and extraordinary refractive index (n_e) of 1.5582; for BK7, thickness of 1 mm and refractive index of 1.5129. In the theoretical fitting, the polyimide (PI) layer was ignored. Due to AR-layer on BK7 in the CLC cell structure (Fig. 3b), the reflectance at each boundary surface of air/AR-layer/BK7/CLC layers was also ignored. At these three incident angles, the measured band position and bandwidth for PBGs were somewhat coincident with theoretical calculations. At oblique incident angle of 50°, the transmission rate was approximately 5% smaller than expected. This seems to be due to optical path that is slightly off the detector, W2.

When comparing results in Fig. 4(a) and Fig. 2, there was another difference between measured data and theoretically fitted data curves near band edges. At a thickness of ~30 μm, measured transmittance values were gently decreased. However, at a thickness of ~10 μm, transmittance values oscillated greatly. In theoretically fitted curves, large oscillations occurred near the band edge at both thicknesses. It seems that in the theoretical calculations, CLC molecules are assumed to form a perfect helical structure regardless of CLC thickness. However, in a real CLC cell with thin thickness, these molecules could be aligned with the perfect helical structure by cooperation between anchoring force of the alignment layer and helical rotary powers of chiral molecules. Therefore, the transmittance oscillated near the band edge (Fig. 2). However, as the film thickness increased, it was harder to form a perfect helical structure due to weak cooperation in the bulk area far from the alignment layer because the helical structure of molecules in the CLC cell originated

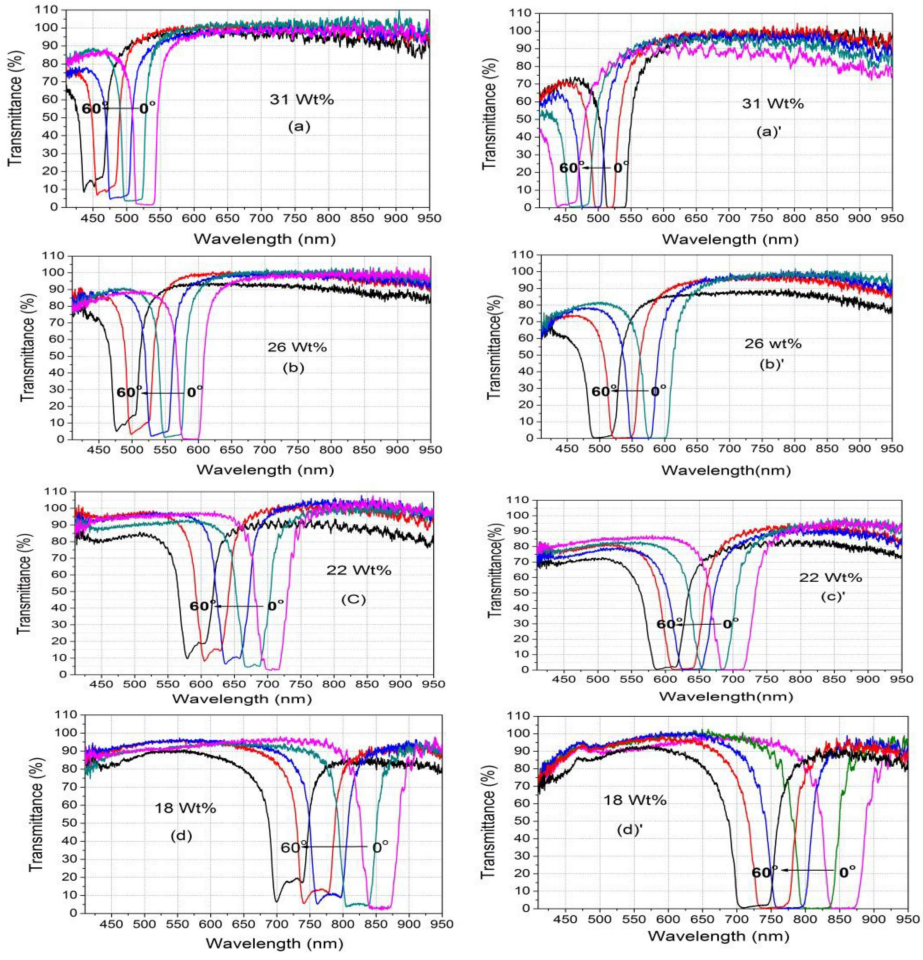

Fig. 5. Continuous blue shifted notch spectra of CLC cells with four different chiral molecular concentrations by rotation from 0° to ∼ 60°. (a), (b), (c), and (d) Curves by rotating one L-CLC cell and one R-CLC cell, respectively. (a)', (b)', (c)', and (d)' Curves by rotating two L-CLC cells and two R-CLC cells with almost the same chiral molecular concentration, respectively.

from the cooperation of the anchoring energy between CLC molecules and the alignment layer (PI) and the helical rotary power of chiral molecules [33]. To apply the CLC cell to a practical filter device, the oscillation near the band edge is a decisive disadvantage. Based on results of this study, an appropriate thickness for the CLC filter would be ∼30 μm. For normal incidence angle data (Fig. 4a), the transmittance decreased from 100% to 95% when wavelength was decreased from 600 nm to a short wavelength due to refractive index mismatch that still existed slightly between the air/AR-layer/BK7/PI/CLC layers, although there was AR coating on BK7.

On the other hand, blue-shifted central wavelengths of the band with an oblique incident angle could be roughly estimated without exact calculations using the 4 × 4 matrix method and the following formula: $\lambda = \mathrm{n} \cdot\ p \cdot \cos\Theta$, $\Theta = \sin^{-1}[(1/n) \cdot \sin(\theta)]$, and $n^2 = (n_e^2 + 2n_o^2)/3$, where λ is incident wavelength, n is average refractive index, p is pitch, θ is incidence angle, n_e is extraordinary and n_o is ordinary refractive index [29]. Experimental (theoretical) central wavelengths of bands were 597 nm (597 nm), 564 nm (563 nm), and 518 nm (514 nm) at incident angles of 0° (□), 30° (○), and 50° (△), respectively [29].

Taken together, these results indicate that a continuously tunable notch filter can be realized by simultaneously rotating L-CLC and R-CLC cells. Fig. 4b shows principle of a notch filter: when an L-CLC and an R-CLC have same PBG wavelength position, for unpolarized incident light, left

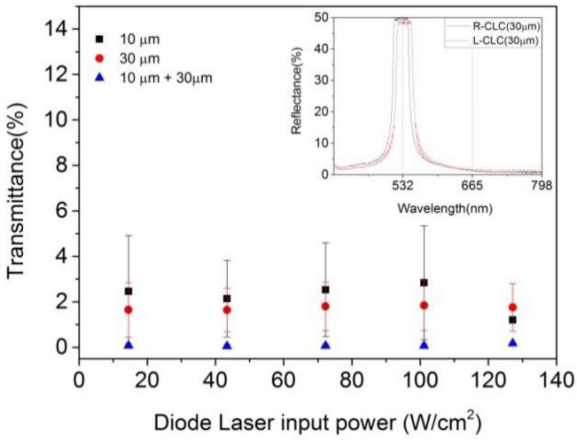

Fig. 6. Transmittance of filters via diode laser power. Data (■), (•), and (▲) are for NF1, NF2, and NF3, respectively. Inset is PBGs of L-CLC (30 μm) and R-CLC (30 μm) cells.

circularly polarized light in the band is reflected at L-CLC and right circularly polarized light in the band is reflected at R-CLC, in turn.

Fig. 5a, b, c, and d show notch spectra that are blue-shifted continuously and the FWHM of the photonic bands that is almost unchanged by rotation from 0° to ∼ 60° after rotating 1-set CLC notches of (L4 and R4), (L3 and R3), (L2 and R2), and (L1 and R1) in the experimental setup (Fig. 3a), respectively.

The transmittance outside the band was almost 70%∼100% in a spectral range. However, as the incident angle increased, light leakage in the band appeared and increased up to ∼10%. For practical applications, the light leakage of ∼10% in the band was not allowed in a notch filter device. As the angle of incidence increased, light leakage in the band appeared and increased, However the rate of the light leakage is smaller in the single CLC cell. To solve this light leakage problem in the band, we applied multiple cell reflection method by using 2-set CLC notches consisted of two L-CLC cells and two R-CLC cells with same PBG position using 2 × (L1 and R1), 2 × (L2 and R2), 2 × (L3 and R3), and 2 × (L4 and R4) cells, respectively. a', b', c', and d' show notch spectra by rotation using 2-set CLC notches. There was no light leakage in the band. Although the transmittance outside the band was decreased to 2∼10%, it is not a problem using it as a notch filter device. Using CLC cells with four different chiral dopant concentrations, spectral range from 440 nm to 870 nm could be covered. Without distortion of the band's shape, each band position of the filter could be determined and controlled reversibly by adjusting rotation angle of the cells. Because each CLC cells has one chiral dopant concentration, they could be permanently stable. One of the problems of LC based devices is the arrangement dependency on temperature. So for the stable operation, one needs to keep ambient temperature constant.

Another important factor for a good filter is that a high laser power can be used without damage the filter if the filter is actually used in a device. To study the stability of filters under operation with high laser power, we used a 532 nm CW Diode laser with maximum power of ∼124 W/cm^2 and a second harmonic generation 532 nm from a Q-switched Nd: YAG laser (pulse width of ∼7 ns, 10 Hz). For power stability study, additionally we made notch filters consisted of an L-CLC (S811, ∼30 wt%) cell and an R-CLC (R811, ∼30 wt%) cell so that the PBG center positions were at ∼532nm. A notch filter 1 (NF1) with ∼10 μm thickness, a notch filter 2 (NF2) with ∼30 μm thickness, and a notch filer 3 (NF3) which consisted of NF1 and NF2 were used.

Fig. 6. shows transmittance of filters operated under various input Diode laser power. Data (■), (•), and (▲) are for NF1, NF2, and NF3, respectively. With high power up to ∼124 W/cm^2, transmittances of NF1 and NF2 were near 2∼3%. Interestingly, the transmittance of NF3 was less than 0.2%. Inset of Fig. 6 shows PBGs of R-CLC (∼30 μm) and L-CLC (∼30 μm) .

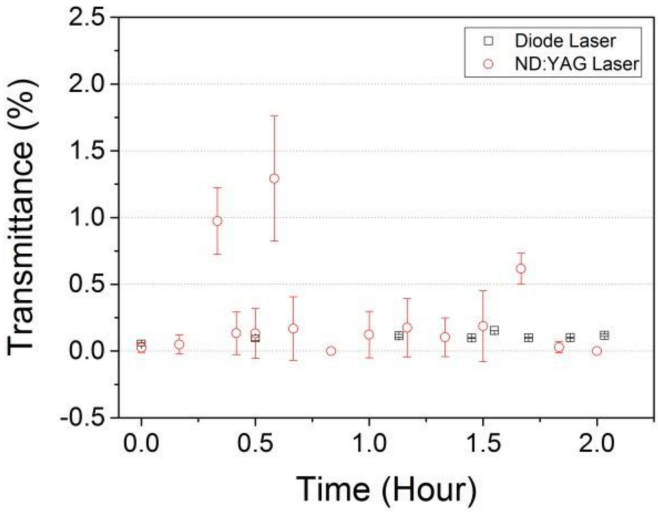

Fig. 7. Stability of transmittance of NF3 after operation at high laser powers for ∼2 hours. Data (○) are for a CW diode laser at ∼124 W/cm^2 power and data (□) are for a pulsed Nd: YAG laser at ∼4.43 MW/cm^2 power.

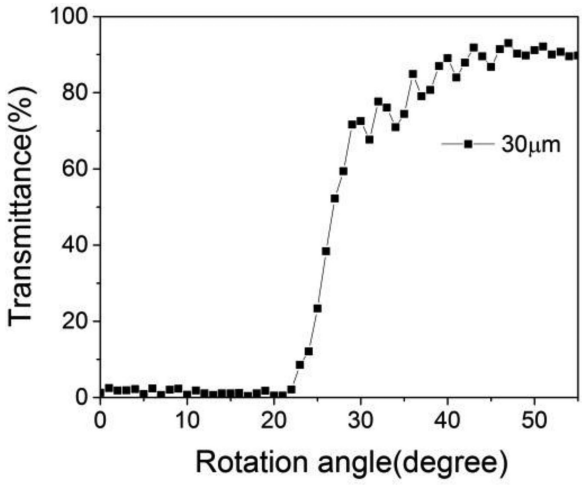

Fig. 8. Transmittance of NF2 via rotation angle for incident 532 nm diode laser at 124 W/cm^2 power.

Fig. 7 shows stability of transmittance of NF3 operated at high laser powers for ∼2 hours. Data (○) are for 532 nm CW diode laser at ∼124 W/cm^2 and data (□) are for pulsed 532 nm Nd: YAG laser at ∼4.43 MW/cm^2 power. Interestingly, after long time exposure under extremely strong laser powers, the transmittance was kept at average less than 0.2%. There was no damage on the filter.

From results shown in Figs. 7 and 8, it can be concluded that the photonic band of the notch filter could also act as a mirror for high power lights. Fig. 8 shows transmittance of NF2 via rotation angle for the 532 nm Diode laser at power of ∼124 W/cm^2. From −22° to 22° incident angle range, it acted as a mirror with ∼98% reflectance. At angles greater than 22°, there was a function of intensity variable beam splitter with varying angles.

4. Conclusions

We developed continuously tunable optical notch filters by combining four left- and right-handed circular CLC cells without subsidiary optical components such as polarizers or phase retarders.

Their optical characteristics were then studied. Filter performance was highly enhanced by introducing an anti-reflection layer to the filter device. By rotating the filter, regardless of the direction of rotation, photonic band positions are continuously blue shifted at spectral range over 100nm. They could be exactly controlled without band deformation. Using four filter sets with four different chiral dopant concentrations, spectral range from 440 nm to 870 nm could be covered. The tuning spectral range could be expanded as much as possible by adjusting the concentration of chiral molecules in CLC. Since each CLC cell has only one chiral dopant concentration, it can secure higher stability in time. Each filter is polarization independent in the spectral range. There was no light leakage inside the photonic band. Outside of the band, transmittance was ∼70%∼100%. In addition, these filters showed stable operation under extremely high laser intensity (∼124 W/cm^2 of CW 532nm diode laser and ∼4.43 MW/cm^2 of Nd: YAG pulse laser) for two hours without showing damage. These filters also have functions of Mirror and intensity variable Beam Splitter. Depending on CLC materials, this simple and easy strategy could be used to prepare filters for applications in optical devices at VIS and NIR spectral range.

Acknowledgment

The authors would like to appreciate Yong-Kuk Yun at Merck Ltd. Korea for supplying MLS-6608, R811, and S811 and Soon-Man Park at Nissan Chemical Korea Co. Ltd. for supplying polyimide (SE-5291).

References

[1] D. Sadot and E. Boimovich, "Tunable optical filters for dense WDM networks," *IEEE Commun. Mag.*, vol. 36, no. 12, pp. 50–55, Dec. 1998.
[2] E. Nicolescu and M. J. Escuti, "Polarization-independent tunable optical filters based on liquid crystal polarization gratings," *Proc. SPIE*, vol. 6654, 2007, Art. no. 665405.
[3] H. R. Morris, C. C. Hoyt, and P. J. Treado, "Imaging spectrometers for fluorescence and raman microscopy: Acousto-optic and liquid crystal tunable filters," *Appl. Spectrosc.*, vol. 48, no. 7, pp. 857–866, 1994.
[4] O. Aharon and I. Abdulhalim, "Design of wide band tunable birefringent filters with liquid crystals," *PIERS Online*, vol. 5, no. 6, pp. 555–560, 2009.
[5] J.-D. Lin *et al.*, "Spatially tunable photonic bandgap of wide spectral range and lasing emission based on a blue phase wedge cell," *Opt. Exp.*, vol. 22, pp. 29479–29492, 2014.
[6] Y. Huang, M. Jin, and S. Zhang, "Polarization-independent bandwidth-variable tunable optical filter based on cholesteric liquid crystals," *Jpn. J. Appl. Phys.*, vol. 53, 2014, Art. no. 072601.
[7] A. Ogiwara and H. Kakiuchida, "Thermally tunable light filter composed of cholesteric liquid crystals with different temperature dependence," *Sol. Energy Mater. Sol. Cells*, vol. 157, pp. 250–258, 2016.
[8] A. Y. Fuh, S. J. Ho, S. T. Wu, and M. S. Li, "Optical filter with tunable wavelength and bandwidth based on phototunable cholesteric liquid crystals," *Appl. Opt.*, vol. 53, pp. 1658–1662, 2014.
[9] E. Oton and E. Netter, "Wide tunable shift of the reflection band in dual frequency cholesteric liquid crystals," *Opt. Exp.*, vol. 25, no. 11, pp. 13314–13323, 2017.
[10] M.-Y. Jeong and J. Y. Mang, "Continuously tunable optical notch filter and band-pass filter systems that cover the visible to near-infrared spectral ranges," *Appl. Opt.*, vol. 57, no. 8, pp. 1962–1966, 2018.
[11] M.-Y. Jeong and J. W. Wu, "Continuous spatial tuning of laser emissions in a full visible spectral range," *Int. J. Mol. Sci.*, vol. 12, no. 12, pp. 2007–2018, 2011.
[12] M.-Y. Jeong and J. Cha, "Firsthand in situ observation of active fine laser tuning by combining a temperature gradient and a CLC wedge cell structure," *Opt. Exp.*, vol. 23, pp. 21243–21253, 2015.
[13] M.-Y. Jeong and J. W. Wu, "Continuous spatial tuning of laser emissions with tuning resolution less than 1 nm in a wedge cell of dye-doped cholesteric liquid crystals," *Opt. Exp.*, vol. 18, pp. 24221–24228, 2010.
[14] M.-Y. Jeong, K. S. Chung, and J. W. Wu, "Optical properties of laser lines and fluorescent spectrum in cholesteric liquid crystal laser," *Nanosci. Nanotechnol.*, vol. 15, pp. 7632–7639, 2015.
[15] V. Joshi, K.-H. Chang, D. A. Paterson, J. M. D. Storey, C. T. Imrie, and L.-C. Chien, "Fast flexoelectro-optic response of bimesogen-doped polymer stabilized cholesteric liquid crystals in vertical standing helix mode," *SID Dig.*, vol. 48, pp. 1849–1852, 2017.
[16] Y. Li, D. Luo, and Z. H. Peng, "Full-color reflective display based on narrow bandwidth templated cholesteric liquid crystal film," *Opt. Mater. Express*, vol. 7, no. 1, pp. 16–24, 2017.
[17] Y. Zhou *et al.*, "Enhanced photonic band edge laser emission in a cholesteric liquid crystal resonator," *Phys. Rev. E*, vol. 74, 2006, Art. no. 061705.
[18] Z.-G. Zheng, B.-W. Liu, L. Zhou, W. Wang, W. Hu, and D. Shen, "Wide tunable lasing in photoresponsive chiral liquid crystal emulsion," *J. Mater. Chem. C*, vol. 3, pp. 2462–2470, 2015.
[19] H. Bian *et al.*, "Optically controlled random lasing based on photothermal effect in dye-doped nematic liquid crystals," *Liq. Cryst.*, vol. 41, pp. 1436–1441, 2014.

[20] A. Chanishvili *et al.*, "Lasing in dye-doped cholesteric liquid crystals: Two new tuning strategies," *Adv. Mater.*, vol. 16, pp. 791–795, 2004.
[21] Y. Huang, L.-P. Chen, C. Doyle, Y. Zhou, and S.-T. Wu, "Spatially tunable laser emission in dye-doped cholesteric polymer films," *Appl. Phys. Lett.*, vol. 89, 2006, Art. no. 111106.
[22] B. Y. Kang, H. H. Choi, M.-Y. Jeong, and J. W. Wu, "Effective medium analysis for optical control of laser tuning in a mixture of azo-nematics and cholesteric liquid crystal," *J. Opt. Soc. Amer. B*, vol. 27, no. 2, pp. 204–207, 2010.
[23] H. Yu, B. Y. Tang, J. Li, and L. Li, "Electrically tunable lasers made from electro-optically active photonics band gap materials," *Opt. Exp.*, vol. 13, no. 18, pp. 7243–7249, 2005.
[24] A. Castellanos-Moreno, P. Castro-Garay, S. Gutiérrez-López, R. A. Rosas-Burgos, A. Corella-Madueño, and J. Adrian Reyes, "Electrically controlled reflection bands in a cholesteric liquid crystals slab," *J. Appl. Phys.*, vol. 106, 2009, Art. no. 023102.
[25] T.-H. Lin *et al.*, "Electrically controllable laser based on cholesteric liquid crystal with negative dielectric anisotropy," *Appl. Phys. Lett.*, vol. 88, 2006, Art. no. 061122.
[26] Q. Hong, T. X. Wu, and S.-T. Wu, "Optical wave propagation in a cholesteric liquid crystal using the finite element method," *Liq. Cryst.*, vol. 30, no. 3, pp. 367–375, 2003.
[27] D. W. Berreman, "Optics in stratified and anisotropic media: 4 × 4 matrix formulation," *J. Opt. Soc. Amer.*, vol. 62, pp. 502–510, 1972.
[28] D. W. Berreman, "Optics in smoothly varying anisotropic planar structures: Application to liquid-crystal twist cells," *J. Opt. Soc. Amer.*, vol. 63, pp. 1374–1380, 1973.
[29] P. G. de Gennes and J. Prost, *The Physics of Liquid Crystals*. Oxford, U.K.: Clarendon, 1993.
[30] M.-Y. Jeong and J. W. Wu, "Temporally stable and continuously tunable laser device fabricated using polymerized cholesteric liquid crystals," *Jpn. J. Appl. Phys.*, vol. 51, 2012, Art. no. 082702.
[31] Y. Wang *et al.*, "Thermally reversible full color selective reflection in a selforganized helical superstructure enabled by a bent-core oligomesogen exhibiting twist-bend nematic phase," *Mater. Horiz.*, vol. 3, pp. 442–446, 2016.
[32] Y.-C. Hsiao, C.-Y. Wu, C.-H. Chen, V. Y. Zyryanov, and W. Lee, "Electro-optical device based on photonic structure with a dual-frequency cholesteric liquid crystal," *Opt. Lett.*, vol. 36, pp. 2632–2634, 2011.
[33] Y.-C. Hsiao, C.-T. Hou, V. Y. Zyryanov, and W. Lee, "Multichannel photonic devices based on tristable polymer-stabilized cholesteric textures," *Opt. Exp.*, vol. 19, no. 24, pp. 23952–23957, 2011.